Key impact of energetic ions on the establishment of advanced tokamak regimes

J. Garcia,[1] J. Citrin,[2,1] G. Giruzzi,[1] P. Maget,[1] M. Schneider,[1] and JET-EFDA contributors[3]
(JET-EFDA, Culham Science Centre, Abingdon, OX14 3DB, UK)
[1] *CEA, IRFM, F-13108 Saint Paul Lez Durance, France*
[2] *Dutch Institute for Fundamental Energy Research DIFFER, Association EURATOM-FOM, Nieuwegein, The Netherlands*
[3] *See the Appendix of F. Romanelli et al., Proc. of the 24th IAEA Fusion Energy Conference 2012, San Diego, USA*

Detailed gyrokinetic and magnetohydrodynamic (MHD) analyses show how a population of energetic ions in a tokamak reduces microturbulence and at the same time improves MHD stability by significantly modifying the pressure profile in the plasma core. For the first time, the key role of energetic particles for the establishment of a positive feedback between plasma core and edge is demonstrated. This effect can enhance the energy confinement in both regions, aiding the further development of advanced scenarios in tokamaks without significant rotation, as will be the case for ITER.

Introduction.– Magnetically confined plasmas are complex nonlinear systems which play a central role in fusion energy research. The energy confinement of magnetic confinement fusion devices like tokamaks is limited by small-scale instabilities (inducing cross-field transport via microturbulence), and by large-scale instabilities that can be described by magnetohydrodynamics (MHD). An important driver of microturbulence is the ion temperature gradient (ITG) mode [1], which becomes linearly unstable if the logarithmic ion temperature gradient exceeds a certain threshold, i.e., for $R/L_{Ti} > R/L_{Ti,crit}$, where $L_{Ti} = T_i/|\nabla T_i|$ is a gradient length and R is the tokamak major radius. Meanwhile, MHD modes significantly restrict the access to high plasma pressure, breaking the magnetic topology at some critical pressure gradient values. Therefore, reducing the impact of these mechanisms is a key challenge in fusion research. Over the years, several kinds of operational regimes (often also referred to as "scenarios") with reduced turbulence have been developed. This includes plasmas with an Internal Transport Barrier (ITB), which have improved energy confinement obtained by the reduction of ITG turbulence in the plasma core in magnetic configurations with reversed safety factor profile or with high enough rotational flow shear [2]. However, due to the large pressure gradients at the ITB location, this scenario often leads to deleterious MHD events. On the other hand, hybrid or advanced inductive scenarios [3], characterized by high confinement and a significant volume of low magnetic shear, have high pressure with limited or few MHD events and therefore may extrapolate to future fusion reactors. The improved confinement is likely due to stability improvements both in the plasma core and at the edge, where a higher pedestal confinement is obtained compared to the standard inductive H-mode scenarios. Improved edge confinement is particularly effective in increasing global confinement, since the pressure peaking factor is maintained due to the logarithmic gradient nature of the critical instability thresholds, a characteristic termed "profile stiffness". Edge and core pressures are thus highly correlated. The dominant impact of increased edge pressure for leading to the high thermal pressure obtained in advanced inductive scenarios has been demonstrated in specific regimes [4]. However, the causality of the process, i.e., whether increased edge stability leads to a higher core pressure, or rather an increase in core pressure induces improved edge stability, has not yet been clarified [5].

While the importance of energetic particles for obtaining advanced scenarios has already been pointed out [6], their exact impact is still not properly understood. Previous linear microinstability analyses have shown that fast ions can stabilize ITG modes in the plasma core due to the dilution of the thermal ions [7], an enhancement of the Shafranov shift [8], or the electromagnetic stabilization due to a local increase of the pressure gradient [9], which may be greatly increased nonlinearly [10]. The impact of fast ion driven geodesic acoustic modes (GAM) has also been highlighted [11]. However, none of these effects can explain the improved confinement in the edge region obtained in advanced inductive scenarios. In this Letter, gyrokinetic and MHD simulations demonstrate, for the first time, that a large population of fast ions is a key ingredient for a positive feedback between plasma core and edge which can improve thermal energy confinement in both regions.

*Modelling methodology.–*A representative discharge of advanced inductive scenarios from JET (#75225) [12] has been analyzed. A summary of the main plasma parameters is found in Tab. I. For this discharge, a high input Neutral Beam Injection (NBI) power is combined with low average density and Greenwald fraction for achieving a high beta, $\beta = 2\mu_0\langle P\rangle/B^2$, and a thermal energy enhancement factor relative to the IPB98(y,2) scaling [13], $H_{98}(y,2)$, above unity. $\langle P\rangle$ is the volume averaged pressure and B the magnetic field. The increase of the ion temperature profile peaking in the core, which significantly exceeds the electron temperature peaking, is a common characteristic in this regime.

An interpretative simulation of the selected discharge

TABLE I. Main characteristics of the discharges analyzed in this letter. I_p is the total current, B_t the toroidal magnetic field, κ the elongation, δ the triangularity, $\beta_N \equiv \beta a B/I_p$ the normalized beta (with a the plasma minor radius), $\beta_{N,th}$ the normalized thermal beta, $H98(y,2)$ the thermal confinement factor, P_{tot} the injected power, and ω_{tor} the toroidal rotation. The JET discharge was analyzed at $t = 6.03s$.

Shot	I_p (MA)	B_t (T)	q_{95}	κ/δ	$\beta_N/\beta_{N,th}$	$H_{98}(y,2)$	P_{tot} (MW)	ω_{tor} (krad/s)
JET 75225	1.7	2.0	4.0	1.64/0.23	3.0/2.13	1.30	17	76.7
ITER	12	5.3	4.30	1.80/0.40	3.0/2.5	1.30	73	∼0

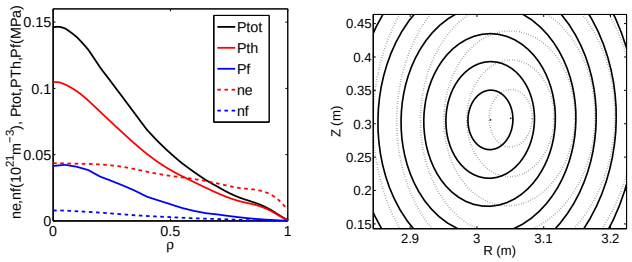

FIG. 1. Total (P_{tot}), thermal (P_{th}), and fast ion (P_f) pressure profiles; electron (n_e) and fast ion (n_f) density profiles (left); magnetic equilibrium without (solid) and with (dot) fast ion content (right) in the JET discharge #75225.

was carried out with the CRONOS [14] suite of integrated modeling codes. The fast ion content for NBI-driven fast ions was calculated by an orbit following Monte Carlo code NEMO/SPOT [15]. The q profile used for the calculations was obtained by equilibrium reconstruction constrained by Motional Stark Effect angles and total pressure. In Fig. 1, the total, thermal, and fast ion pressures, as well as the fast ion and electron density profiles, and the magnetic equilibrium are shown. The fast ions change the total plasma energy content by changing the core pressure profile, which modifies the normalized beta from $\beta_{N,th}^{75225} = 2.13$ to $\beta_N^{75225} = 3.0$. This has a strong impact on the magnetic equilibrium and, in particular, on the Shafranov shift which increases to $\Delta_{75225}^{Shafranov-Shift} \approx 4.0$ cm. The ratio of thermal and fast ion densities is also modified as $n_{fast}/n_e \sim 0.13$ at $\rho = 0.33$. Finally, the pressure gradient in the core region is strongly modified. A parameter of merit of the local pressure modification is $\alpha \equiv -Rq^2 d\beta/dr$, which increases from $\alpha_{th}^{75225}(\rho = 0.33) = 0.35$ up to $\alpha^{75225}(\rho = 0.33) = 0.52$.

In order to analyze the impact of fast ions, the gyrokinetic code GENE [16] and the MHD code MISHKA [17] were used to compute, respectively, microturbulence in the core and ideal MHD stability at the edge. The MHD equilibrium code HELENA [18] was used to solve the Grad-Shafranov equation with and without fast ions. For the gyrokinetic analysis, all simulations included kinetic electrons, collisions, electromagnetic effects, and the fast ions as a separate active species. The geometry used was calculated by HELENA based on the interpretative analysis of the discharge. The instability linear growth

TABLE II. Discharge dimensionless parameters at $\rho = 0.33$.

Shot	$\hat{s}$	q	T_e/T_i	R/L_{Ti}	R/L_{Te}	R/L_{ne}
75225	0.15	1.16	0.67	6.0	4.3	2.6
ITER	0.24	1.17	1.09	3.4	2.9	1.9

rates γ and flow shear rate, γ_E, are in units of c_s/R, with $c_s \equiv \sqrt{T_e/m_i}$ and m_i the main ion mass. Both $\delta B_\perp$ and $\delta B_\parallel$ fluctuations were computed as they can both play a significant role in high β discharges [19]. The fast ion distribution function was approximated as a Maxwellian, taking the average energy of the fast ion slowing-down distribution as the temperature, which is found to be $T_{fast} = 35$ keV. For the gyrokinetic calculations excluding the fast ions, the equilibrium was recalculated with only the thermal pressure. The peeling-ballooning diagram was calculated following the procedure detailed in Ref. [20]. In this case, as previously, the equilibrium was calculated with and without fast ions in order to analyze the ideal MHD modes for both cases. The dimensionless parameters of the discharge at $\rho = 0.33$ fed into the gyrokinetic calculations are summarized in Tab. II. The selected time for the discharge 75225 is t=6.03s, in which the performance is maximized and no deleterious core MHD is detected [12].

Simulation results.– In Fig. 2, the linear growth rates and frequencies are shown for the nominal experimental value of $R/L_{Ti} = 6.0$ as well as for an increased value of $R/L_{Ti} = 7.2$ to test the sensitivity within the confidence interval. In order to identify the nature of the underlying modes, the flow shear rate was set to zero. ITG modes are found over a wide wavenumber range at $R/L_{Ti} = 6.0$, whose maximum growth rate is reduced by 32% when including the fast ions.

The influence of electromagnetic effects, which can stabilize ITG modes [21], was analyzed. This was confirmed by performing an electrostatic simulation, reducing the electron beta, $\beta_e = 2\mu_0\langle P_e\rangle/B^2$, from the nominal value of 1.6% to zero, which lead to a significant increase of the linear growth rates. For $R/L_{Ti} = 7.2$, in addition to ITG modes, modes drifting in the ion diamagnetic direction but possessing a higher frequency, $c_s/R = 2.5$, appear for $0 < k_y < 0.25$. These modes can correspond to β-induced Alfvén Eigenmodes (BAEs) [22], which oscillates with the GAM frequency, and which are known to be destabilized by the presence of high energetic particles pressure gradients [23]. Therefore, at this radial position, the turbulence regime is found to be in the direct vicinity of the ITG-BAE boundary. Next, we carried out a nonlinear R/L_{Ti} scan with and without fast ions. The experimental toroidal rotation was taken into account by including the $E \times B$ flow shear rate, $\gamma_E = 0.2$. The heat flux obtained is normalized by the factor $q_{GB} = {T_i}^{2.5} n_i {m_i}^{0.5}/e^2B^2R^2$, where n_i is the ion density. The experimental ion heat flux, obtained by power balance, is found to be consistent with

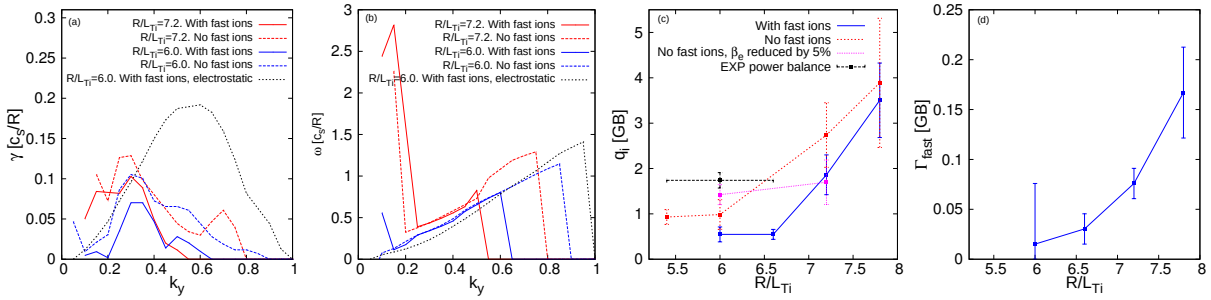

FIG. 2. Linear growth rates and frequencies for discharge 75225 (a,b) Ion heat flux and fast ions particle flux from nonlinear gyrokinetic simulations (c,d). The analysis was carried out at $\rho = 0.33$.

the calculations. Here, the fast ions provide an improvement of $\sim 10-20\%$ on R/L_{Ti} for the same heat flux. When $R/L_{Ti} > 7.2$, the heat flux rapidly increases beyond the experimental value, and the fast ions are no longer stabilizing. At that moment, the fast ion transport also rapidly increases, something that confirms the fact that the high frequency electromagnetic modes found at $R/L_{Ti} = 7.2$ are BAE as they have a strong resonant interaction with both thermal ions and energetic particles. It is worth pointing out that since the BAE limit depends also on the fast ion pressure gradients, this fast ion transport increase in the BAE regime may lead to a self-limitation mechanism whereby the fast ion pressure gradient is maintained at a level consistent with BAE marginality. However, flux-driven simulations with self-consistent profile evolution would be necessary to ascertain this conjecture.

We now analyze the edge stability. In the peeling-ballooning diagram shown in Fig. 3, the boundary of the stable region is extended by including the fast ions which leads to a pedestal pressure increase of $\sim$10% in the ballooning region (i.e. the region limited by the pressure gradient in which the experimental pressure is obtained). This shows the favorable impact of β on the edge stability through the Shafranov shift, as obtained from the analysis of DIII-D and JT-60U [4, 24]. It is worth pointing out that, due to the plasma stiffness, even a modest improvement of the pedestal can lead to a higher overall improved thermal confinement compared with solely improving the core microturbulence as the volume affected is much higher. Since the nonlinear electromagnetic stabilization is expected to be stronger than its linear counterpart due to increased coupling to zonal flows [25], the impact of higher electron core pressure (or β_e) in the core turbulence, due to a change in the pressure pedestal, can be quite important. A rough analysis of the interplay between core and edge has been studied by performing again the nonlinear simulations at $R/L_{Ti} = 6.0$ and $R/L_{Ti} = 7.2$ without the fast ion population but considering 5% lower β_e, assuming that the 10% reduction of pedestal pressure obtained by removing the fast ion content leads to a 5% less electron pressure in the core through stiffness. As shown in Fig. 2, at $R/L_{Ti} = 6.0$, the heat flux increases by 25% due to lower electromagnetic stabilization of ITG modes, however, at $R/L_{Ti} = 7.2$, the flux actually decreases since the lower pressure leads to the stabilization of BAE.

In order to demonstrate that the fast ions are indeed a key ingredient for both a microturbulence improvement in the core and a pedestal pressure enhancement at the edge, an alternative gyrokinetic calculation was carried out. The fast ion content was removed and the thermal electron and ion content and gradients were increased such that β_N and α are maintained, whereas the plasma geometry is also kept constant. In these two cases, the pedestal would behave exactly the same since the Shafranov shift is the same. The new growth rates, shown in Fig. 3, increase throughout the spectrum, and its maximum is 2.5 times higher compared to the case with fast ions hence potentially resulting in a much larger heat flux. The key point is that the fast ions, unlike thermal particles, increase the pressure in the plasma core, while simultaneously not contributing to the ITG drive and even reducing it (which can lead to higher thermal pressure as the ion temperature also increases). Therefore under the same conditions, in particular for the same input power, a particular level of Shafranov shift (or of pedestal improvement) is achieved much more efficiently in the presence of a high fast ion population than with pure thermal particles. Increased thermal content also increases core microturbulence limiting the global β obtained and therefore also limiting the possible pedestal pressure attained. This can also be part of the explanation of the well-known improvement of the pedestal pressure with power [26]. This mechanism is expected to be efficient until the destabilization of BAE due to high core pressure gradients. At that point, the core-edge feedback is saturated from the core side.

With the aim of analyzing if the same effect can play a role in tokamaks with low external torque, as ITER [27], the same procedure has been applied to a typical ITER hybrid scenario [28] with the characteristics shown in Tab. I. Although the fast ion densities associated with the fusion α-particles and with the NBI beams are low,

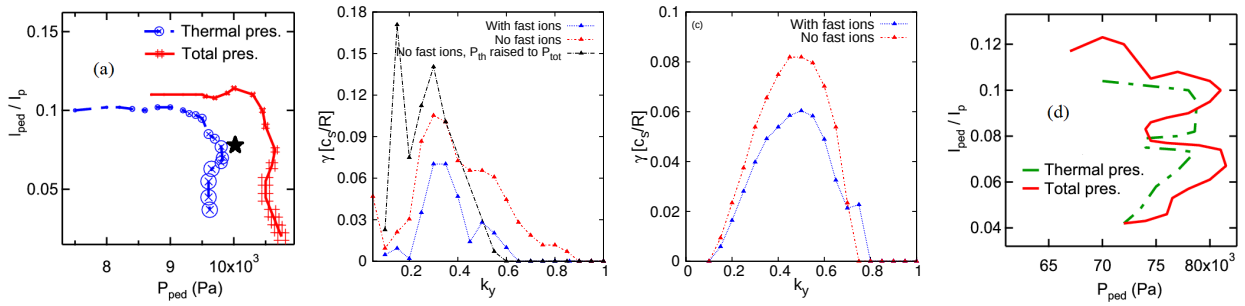

FIG. 3. Peeling-ballooning boundaries for discharge 75225. The experimental value is marked with a star (a). Linear growth rates with and without fast ions and with artificially increased thermal pressure (b). Linear growth rates with and without fast ions for the ITER hybrid scenario at at $\rho = 0.33$ (c). Peeling-ballooning boundaries with and without fast ions for ITER (d).

$n_{fast,\alpha}/n_e \sim 0.009$ and $n_{fast,beams}/n_e \sim 0.006$, their pressure is not negligible as their energy is quite high, $T_{fast,\alpha} = 1.1$ MeV and $T_{fast,beams} = 0.55$ MeV which increases $\beta_{N,th} = 2.5$ up to $\beta_N = 3.0$. Microturbulence, calculated at $\rho = 0.33$, is found to be ITG-driven (although close to BAE modes) and also modified by these fast ions with a growth rate reduction of up to 30%. The increased β also expands the stable peeling-ballooning region at the edge in a similar way as obtained for JET (up to 10%). This represents a significant increase of 18% in the fusion power, which in turn increase β in a positive feedback loop. This implies that, unlike rotational flow shear, the role played by fast ions in ITER and future tokamak reactors can have the same impact as in present day experiments, primarily due to the α-particles, which will be the main heating mechanism.

Summary.–We have presented evidence of the simultaneous modification by fast ions of core microturbulence and edge MHD. The fast ions increase the total core pressure without increasing the turbulence drive, and can even reduce the ITG microturbulence. This leads to an improved edge pedestal pressure by means of the increased Shafranov shift in a manner unachievable by pure thermal pressure, which is strongly limited by microturbulence. A positive core-edge feedback is therefore established due to stiffness which increases central electron pressure and can stabilize even more ITG modes because of the electromagnetic effects. This loop is expected to be efficient until the fast ion pressure gradient destabilizes BAE which strongly increase both thermal and fast ion transport. In ITER and fusion reactors, this effect can play a similar role as in present day experiments, owing to the high level of fast ions born from fusion reactions, and therefore can compensate for the low rotation expected due to the high density required for producing sufficient fusion energy.

Acknowledgements.–This work, supported by the European Communities under the contract of Association between EURATOM and CEA, was carried out within the framework of the European Fusion Development Agreement. The views and opinions expressed herein do not necessarily reflect those of the European Commission. Discussions with C. Challis, N. Hayashi and S. Ide are highly appreciated.

[1] F. Romanelli, Phys. Fluids B **1**, 1018 (1989).
[2] J.W. Connor *et al.,* Nucl. Fusion **44**, R1 (2004).
[3] T.C. Luce *et al.,* Nucl. Fusion **43**, 321 (2003).
[4] Y. Kamada *et al.,* Plasma Phys. Control. Fusion **44**, A279-A286 (2002).
[5] C.F. Maggi *et al.,* Nucl. Fusion **47**, 535 (2007).
[6] J. Garcia, G. Giruzzi Nucl. Fusion **53**, 043023 (2013).
[7] G. Tardini *et al.,* Nucl. Fusion **47**, 280 (2007).
[8] C. Bourdelle, G.T. Hoang, X. Litaudon, C.M. Roach and T. Tala, Nucl. Fusion **45**, 110 (2005).
[9] M. Romanelli, A. Zocco, F. Crisanti, and JET-EFDA Contributors, Plasma Phys. Control. Fusion **52**, 045007 (2010).
[10] J. Citrin *et al.,* Phys. Rev. Lett. **111**, 155001 (2013).
[11] D. Zarzoso *et al.,* Phys. Rev. Lett. **110**, 125002 (2013).
[12] J. Hobirk *et al.,* Plasma Phys. Control. Fusion **54**, 095001 (2012).
[13] ITER Physics Basis, Nucl. Fusion **39**, 2175 (1999).
[14] J.F. Artaud *et al.,* Nucl. Fusion **50**, 043001 (2010).
[15] M. Schneider, L.-G. Eriksson, I. Jenkins, J.F. Artaud, V. Basiuk, F. Imbeaux, T. Oikawa, JET-EFDA contributors, and ITM-TF contributors, Nucl. Fusion **51**, 063019 (2011).
[16] F. Jenko, W. Dorland, M. Kotschenreuther, and B.N. Rogers, Phys. Plasmas **7**, 1904 (2000); see http://gene.rzg.mpg.de for code details and access.
[17] G.T.A. Huysmans *et al.,* Plasma Phys. Control. Fusion **8**, 4292 (2001).
[18] G.T.A. Huysmans *et al.,* CP90 Conference on Comp. Physics, Word Scientific Publ. Co. 1991, p.371.
[19] E.A. Belli , J. Candy, Phys. Plasmas **17**, 112314 (2010).
[20] P. Maget *et al.,* Nucl. Fusion **53**, 093011 (2013).
[21] J.Y. Kim, W. Horton and J.Q. Dong, Phys. Fluids B **5**, 4030 (1993).
[22] W. W. Heidbrink *et al.*,Phys. Rev. Lett. **71**, 855 (1993).
[23] F. Zonca *et al.,* Plasma Phys. Controlled Fusion **38**, 2011 (1996).
[24] P. Snyder *et al.,* Nucl. Fusion **47**, 961 (2007).
[25] M.J. Pueschel, T. Görler, F. Jenko, D.R. Hatch, and A.J.

Cianciara Phys. Plasmas **20**, 102308 (2013).
[26] D.C. Mcdonald *et al.,* Nucl. Fusion **47**, 147 (2007).
[27] R.V. Budny *et al.,* Nucl. Fusion **48**, 075005 (2008).
[28] K. Bassiguir *et al.,* Plasma Phys. Control. Fusion **55**, 125012 (2013).